ELSEVIER

Journal of Photochemistry and Photobiology A: Chemistry 115 (1998) 213–221

Journal of Photochemistry and Photobiology A:Chemistry

Photodynamic action of a water-soluble hypocrellin derivative with enhanced absorptivity in the phototherapeutic window I: ESR and UV–Vis studies on the photogeneration of the semiquinone anion radical and hydroquinone

Yu-Ying He, Jing-Yi An, Li-Jin Jiang *

Institute of Photographic Chemistry, Academia Sinica, Beijing 100101, China

Received 6 January 1998; received in revised form 27 February 1998; accepted 7 April 1998

Abstract

Cysteine-substituted hypocrellin B (Cys-HB) is a hypocrellin derivative with enhanced water solubility and absorption in the domain of phototherapeutic window (600–900 nm). Illumination of Cys-HB in DMSO or DMSO-buffer (pH 8.0) generated a strong Electron Spin Resonance (ESR) signal. The ESR signal was assigned to the semiquinone anion radical of Cys-HB (Cys-HB$^{\bullet -}$) based on a series of experimental results. Decay of Cys-HB$^{\bullet -}$ in the presence and absence of electron donors, were both consistent with second-order kinetics. Spin counteraction of TEMPO by Cys-HB photosensitization indicated the formation of Cys-HB$^{\bullet -}$ which couldn't be detected by ESR method directly in aqueous solution or acidic media. Spectrophotometric measurements showed that the absorption bands at 623 nm, and 504 nm (pH 8.0) or 520 nm (pH 11.0) were those of Cys-HB$^{\bullet -}$ and hydroquinone of Cys-HB (Cys-HBH_2), respectively. The kinetical results of Cys-HB$^{\bullet -}$ decay were in agreement with those by ESR measurements. Compared with hypocrellin B (HB), Cys-HB$^{\bullet -}$ was more stable and less susceptible in strong alkaline media. Strong intramolecular hydrogen bonding was considered to be present in the chromophore of Cys-HB$^{\bullet -}$. The results in this study showed that Cys-HB was at least a favorable Type I phototherapeutic agent.

Keywords: Cysteine-substituted hypocrellin B; Semiquinone anion radical; Hydroquinone; ESR spectra; Spin counteraction; Spectrophotometric measurements

1. Introduction

Hypocrellin A (HA) and hypocrellin B (HB, Fig. 1) are new types of photosensitive pigments and medicines, which derive their names from *Hypocrella bambuase* (B. et Br) sacc, a parasitic fungus of *Sinarundinaria* sp. growing abundantly in the northwestern region of Yunnan in China. Photophysical, photochemical and photobiological properties of hypocrellins have been studied extensively and reviewed [1–4]. These lipid-soluble perylenequinonoid compounds were selected as potential photosensitizers for photodynamic therapy (PDT) owing to their high quantum yields of singlet oxygen ($^1O_2$), substantial absorption in the red spectral region, availability in pure monomeric form and facility for site-directed chemical modifications to optimize properties of red light absorption, tissue biodistribution and toxicity [5]. Recently, substantial advances have been made on various aspects of hypocrellins and their derivatives, the most intriguing being their activities against cancers and the acquired immunodeficiency syndrome (AIDS). Miller and coworkers [5–9] have investigated the in vitro cyto and phototoxicity, acute and chronic toxicity in vivo, intracellular uptake kinetics and distribution, pharmacokinetics, pH and oxygen dependency, tumoricidal activity, cutaneous photosensitivity and genotoxicity of hypocrellins and their derivatives. Of all ethanolaminated HB and butylaminated HB elicit phototoxicity in vitro primarily via Type II mechanism, with some Type I activity under stringently hypoxic conditions. It was found that some animated hypocrellins exhibit even more preferential lysosomal localization than their parent hypocrellins, which can be used to enhance the drug selectivity [5–8]. The in vivo studies have indicated that hypocrellin B has a qualitatively similar tissue distribution pattern to that of Photofrin II, but with faster kinetics [5–9]. A significant finding is the rapid clearance rate of hypocrellin B from plasma and full incorporation into murine tumor within 2 h of intravenous administration. This might be the reason why

* Corresponding author.

1010-6030/98/$19.00
PII S1010-6030(98)00273-1

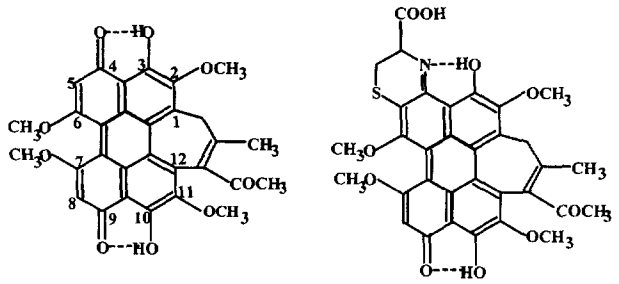

Fig. 1. Chemical structures of HB (left) and Cys-HB (right).

hypocrellins generally exhibit much less delayed skin photosensitization in both animals and humans than porphyrins such as Photofrin II. Hudson et al. [10,11] have demonstrated that hypocrellins inactivates HIV-I almost as efficiently as hypericin does [10], herpes simplex virus type 1 and Sindbis virus demonstrating the correlation between quantum yield of singlet oxygen ($^1O_2$) by hypocrellins and antiviral efficiency [11] in the presence of visible light. In addition, a number of hypocrellins and their analogs have been observed to be potent inhibitors of protein kinase C (PKC), a key enzyme in cellular differentiation and proliferation, via Type I and/or Type II photosensitization [12]. And hypocrellin A has been used to probe artherosclerotic deposits via a laser-induced fluorescence-guided angioplasty system [13].

However, natural hypocrellins are insoluble in water and, as in the case of natural HPD, rarely exhibit absorptivity longer than 600 nm sufficiently strong for PDT. These disadvantages prevent further investigations on their biological consequences and limit their PDT application clinically. Accordingly, we report the preparation of cysteine-substituted hypocrellin B (Cys-HB, Fig. 1), which demonstrates enhanced water solubility and red absorptivity (Fig. 2).

The semiquinone anion radical of hypocrellin was considered to be a key intermediate in the cytotoxic reactions through the ability of this radical to generate toxic species such as active oxygen ($O_2^{\bullet -}$, H_2O_2, and HO•) in the presence of oxygen and its direct participation in the reaction with the substrates in the absence of oxygen [14–17]. And it has been shown that not only the active oxygen species ($^1O_2$, $O_2^{\bullet -}$ and HO•) but also the quinone radical (anion radical and cation radical) participate in the photodynamic damage caused by HA [14,18]. The hydroquinone might also play an important role in the cytotoxic reactions, since it can be oxidized to generate semiquinone anion radical and active oxygen species via one electron oxidation. Cysteine-substituted hypocrellin B (Cys-HB) derivative possesses both enhanced water-solubility and red absorptivity in the domain of phototherapeutic window (600–900 nm), so investigations in detail on the photochemical and spectroscopic properties, and the kinetics of Cys-HB radical and hydroquinone (Cys-HBH_2) are of critical importance made in this paper. And the identification of Cys-$HB^{\bullet -}$ and Cys-HBH_2 and the effects of different media are reported herein.

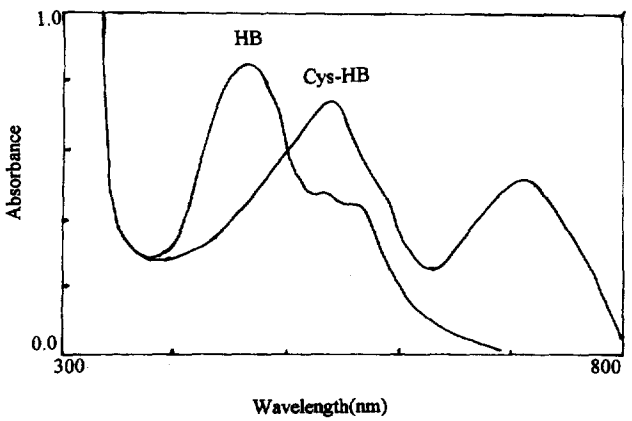

Fig. 2. Absorption spectra of HB and Cys-HB.

2. Material and methods

2.1. Chemicals

HA was extracted from fungus sacs of *H. bambuase* and purified by recrystallization twice from acetone. HB was prepared from dehydration of HA [19]. 5,5-Dimethyl-1-pyrroline-*N*-oxide (DMPO) and 2,2,6,6-tetramethyl-4-piperidone-*N*-oxyl radical (TEMPO) were obtained from Aldrich Chemical. Cysteine, reduced glutathione, reduced nicotinamide adenine dinucleotide (NADH) and superoxide dismutase (SOD) were purchased from Biotech Technology, Chinese Academy of Sciences (China). Sodium sulfite and other agents of analytical grades were obtained from Beijing Chemical Plant (China). DMPO was purified with activated charcoal prior to use. The solutions were purged with argon, air or oxygen according to the experimental requirements.

2.2. Preparation of cysteine-substituted hypocrellin B (Cys-HB)

Cys-HB was prepared according to the method of He et al. [20], by photolysis of ethanol-buffer (1:3 by volume, pH 11) solution containing HB (0.2 mM) and cysteine (10 mM). A medium-pressure sodium lamp (450 W) was used as light source and filters were used to cut off light of wavelength shorter than 470 nm. A water-jacketed cooling device was applied to maintain the temperature at 20°C. The reaction mixture was irradiated for about 15 min, followed by neutralization with 10% hydrochloric acid, chloroform extraction and vacuum evaporation to afford colored solid. The solid was subjected to 1% citric acid-silica gel thin-layer chromatography, using a 98:2 mixture of chloroform and methanol as developing agent and acetone as eluent.

2.3. ESR measurement

Electron Spin Resonance (ESR) spectra were recorded at room temperature, using a Bruker ESP-300E spectrometer operating at 9.80 GHz, X-band with 100 kHz field modula-

tion. Samples (40 μl) were injected into quartz capillaries specially made for ESR analyses. Samples were irradiated in the cavity by using a 1 kW Xenon arc lamp with a long pass filter to eliminate light of wavelength shorter than 540 nm. The incident fluence rate at the cavity window was approximately 23 W m^{-2}. ESR spectra were recorded, stored and manipulated by using an IBM/PC computer.

2.4. UV–Vis measurement

Absorption spectra were conducted on a Hewlett-Packard 8541A diode array spectrometer, using solution of Cys-HB (60 μM) or HB (40 μM). The productions of the semiquinone anion radical and hydroquinone of Cys-HB were measured by the decreases in absorbance at 538 nm, and 623 nm which was assigned to the Cys-HB anion radical (see below), respectively.

3. Results and discussion

3.1. ESR measurements of free radical produced during photosensitization of Cys-HB anaerobically

Irradiation of Cys-HB (1 mM) in deoxygenated dimethylsulfoxide (DMSO) solution for 2 min generated the hyperfine spectrum shown in Fig. 3A, with $g=2.0085$. The intensity of the signal was dependent on irradiation time and intensity, and increased during the photolysis and decreased slowly in the dark (the inset A in Fig. 3). The ESR signal intensity of Cys-HB radical also depended on the concentration of Cys-HB and increased with the Cys-HB concentration (the inset B in Fig. 3). The strong concentration effect indicated that the Cys-HB radical might be formed via self-electron transfer between the excited and ground species according to Ref. [21].

$$\text{Cys-HB}^{\star}+\text{Cys-HB}\rightarrow\text{Cys-HB}^{\bullet-}+\text{Cys-HB} \quad (1)$$

3.1.1. Identification of the photogenerated Cys-HB radical

In order to identify the ESR signal shown in Fig. 3A, the following experiments were carried out.

(1) NADH (5 mM), a typical electron donor (D), was added to the deoxygenated DMSO solution containing Cys-HB (1 mM) irradiated for 30 s. The ESR spectrum obtained (Fig. 3B) was similar to that obtained in the absence of NADH (Fig. 3A), and the presence of NADH intensified the ESR signal significantly. Meanwhile the color of the sample changed from bluish purple (the color of Cys-HB, Fig. 2) to cyan ascribed to the Cys-HB radical thus generated. The electron transfer from electron donor (D) to excited Cys-HB generated the semiquinone anion radical of Cys-HB (Cys-$HB^{\bullet-}$) shown in Eq. (2). This indicated the anionic characteristics of the Cys-HB radical shown in Fig. 3B and thus Fig. 3A.

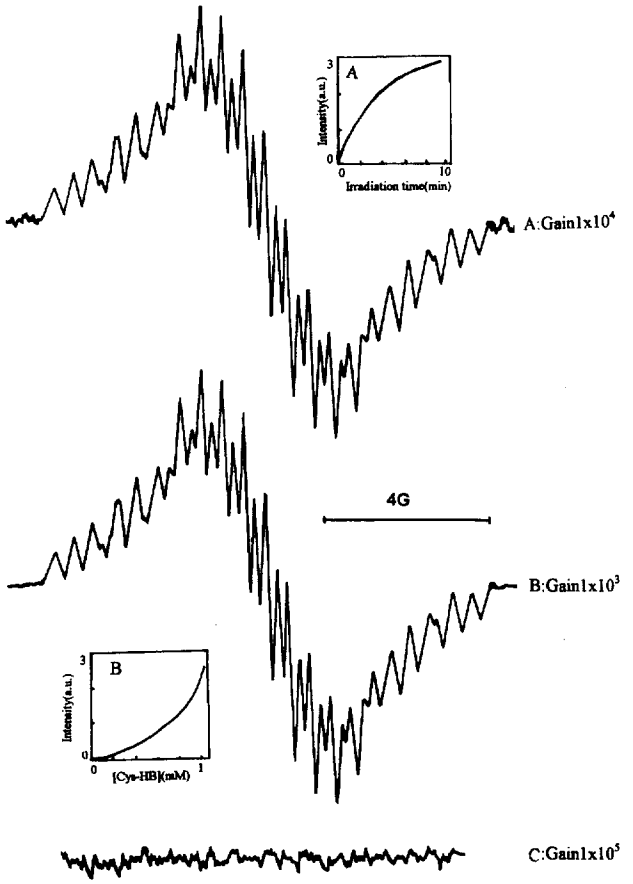

Fig. 3. (A) Photoinduced ESR spectrum from the deoxygenated DMSO solution of Cys-HB (1 mM). Illumination continued for 2 min with visible light. (B) Photoinduced ESR spectrum from the deoxygenated DMSO-buffer (1:1 by volume, pH 8.0) solution of Cys-HB (1 mM) and NADH (5 mM). (C) As in (A) but oxygen was bubbled through the solution after illumination. Instrumental settings: microwave power, 8 mW; modulation amplitude, 0.08 G; sweep width, 20 G; receiver gain, 1×10^4. Inset A shows the ESR signal intensity of Cys-HB radical as a function of irradiation time; inset B shows the ESR signal intensity of Cys-HB radical as a function of Cys-HB concentration (instrumental settings: microwave power, 8 mW; modulation amplitude, 0.08 G; sweep width, 20 G; receiver gain, 1×10^5) (a.u., arbitrary units).

$$\text{Cys-HB}^{\star}+\text{D}\rightarrow\text{Cys-HB}^{\bullet-}+\text{D}^{\bullet+} \quad (2)$$

(2) A series of other electron donors (D) with different redox potentials were added to the Cys-HB solution in place of NADH. In all cases, the ESR signals of Cys-HB radical were intensified with similar spectra as compared with that obtained in the absence of electron donors after illumination for 2 min (Table 1). Table 1 also showed that the intensity increased sharply with the decrease in the redox potentials of the donors added. This further confirmed the anionic nature of the Cys-HB radical.

(3) The ESR signal of the Cys-HB radical shown in Fig. 3A was quenched completely by the purge of oxygen, as shown in Fig. 3C. Moreover, when DMPO and oxygen were introduced into the irradiated Cys-HB radical solution, the ESR signal of DMPO-superoxide radical adduct (Fig. 4A) appeared immediately, accompanied by the disappearance of

Table 1
Effect of electron donors with different redox potentials on the intensity of the ESR signal intensity of Cys-HB radical

Electron donor	Relative intensity	$E_{(D^{\cdot+}/D)}$ (V)
Cys-HB	1	–
Glutathione	62	0.87
Cysteine	135	0.63
Na_2SO_3	140	0.63
NADH	282	0.28

The DMSO-buffer (1:1 by volume, pH 8.0) solution containing Cys-HB (1 mM) and electron donor (5 mM) was irradiated for 2 min. Instrumental settings: microwave power, 3 mW; modulation amplitude, 1 G.

the ESR signal of Cys-HB radical. The spectroscopic parameters for Fig. 4A were determined to be $a^N = 13.0$ G, $a_\beta^H = 10.5$ G and $a_\gamma^H = 1.30$ G, and were close to those reported previously for DMPO-superoxide radical adduct [15,22]. In the presence of SOD, the ESR signal shown in Fig. 4A was inhibited and the degree of inhibition increased as the concentration of SOD increased (Fig. 4B), which further confirmed the formation of superoxide anion radical detected by the DMPO spin trap. As a quencher, oxygen accepted one electron from Cys-HB$^{\cdot-}$ to form $O_2^{\cdot-}$ via Eq. (3), resembling the parent hypocrellins [23]. This suggested that the ESR signal shown in Fig. 3A should be ascribed to the semiquinone anion radical of Cys-HB (Cys-HB$^{\cdot-}$) rather than other species such as Cys-HB cation radical, similar to hypocrellin A [23].

$$\text{Cys-HB}^{\cdot-} + O_2 \rightarrow \text{Cys-HB} + O_2^{\cdot-} \quad (3)$$

In accordance with the above results, the ESR spectrum in Fig. 3A can be safety assigned to the semiquinone anion radical of Cys-HB (Cys-HB$^{\cdot-}$).

3.1.2. Dark decay kinetics of the semiquinone anion radical of Cys-HB (Cys-HB$^{\cdot-}$)

The ESR signal intensity of Cys-HB$^{\cdot-}$ decreases in the dark after illumination was stopped. The kinetics of dark decay of Cys-HB$^{\cdot-}$ was measured by recording the decrease in the amplitude of the ESR signal from its steady state level after illumination was stopped. The result were shown in Fig. 5. The decay in the presence of electron donor such as NADH (5 mM) in deoxygenated DMSO-buffer (1:1 by volume, pH 8.0) solution shown by line A was consistent with second-order kinetics. Line B showed the decay plot of Cys-HB$^{\cdot-}$ in DMSO in the absence of electron donor, which was similar to line A, i.e., consistent with second-order kinetics, but with a much slower decay rate than line A. In the absence of electron donor, Cys-HB$^{\cdot-}$ decayed via Eq. (4), i.e., the disproportionation of the anion radical generated via Eq. (1), following the second-order kinetics. In the presence of electron donor, Cys-HB$^{\cdot-}$ generated via Eq. (2) might decay via Eq. (4) or/and Eq. (5) corresponding to the second-order kinetics and the first-order kinetics, respectively. The consistence of Cys-HB$^{\cdot-}$ decay with second-order kinetics suggested that the decay via Eq. (4) was predominant under our experimental conditions.

$$\text{Cys-HB}^{\cdot-} + \text{Cys-HB}^{\cdot-} \xrightarrow{H^+} \text{Cys-HBH}_2 + \text{Cys-HB} \quad (4)$$

$$\text{Cys-HB}^{\cdot-} + D \xrightarrow{H^+} \text{Cys-HBH}_2 + D^{\cdot+} \quad (5)$$

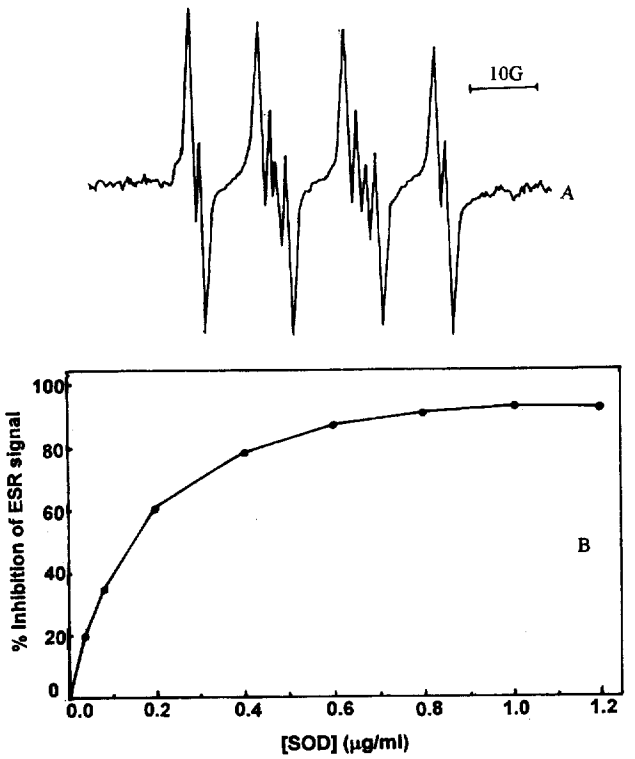

Fig. 4. (A) ESR spectrum of DMPO-superoxide radical adduct obtained after DMPO (50 mM) and oxygen were involved in the Cys-HB radical solution. The Cys-HB solution was obtained by photolysis of Cys-HB with NADH as electron donor. (B) Inhibition of DMPO-$O_2^{\cdot-}$ ESR signal by adding different concentrations of SOD. Instrumental settings: microwave power, 8 mW; modulation amplitude, 1 G; scan range, 200 G; receiver gain, 1×10^4).

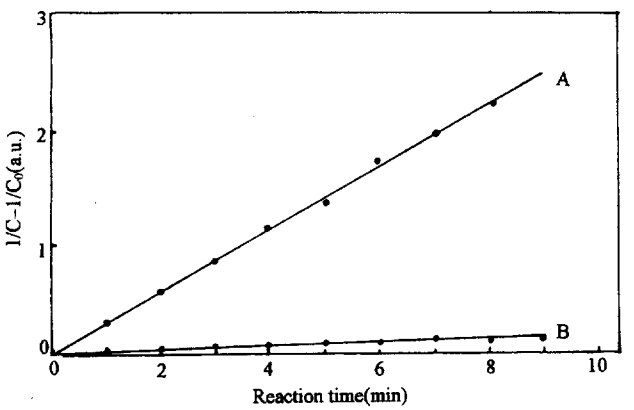

Fig. 5. Dependence of the reciprocal of the Cys-HB semiquinone anion radical concentration (C) on the time of dark reaction. Line A: in the presence of NADH (5 mM) in DMSO-buffer (1:1 by volume, pH 8.0); line B: in the absence of NADH in DMSO. (Instrumental settings: microwave power, 8 mW; modulation amplitude, 0.08 G; sweep width, 20 G; receiver gain, 1×10^5).

The decay process of Cys-HB$^{\bullet -}$ could also be observed by the color changes of the sample. The color of the sample in the presence of NADH (5 mM) changed from bluish purple (the color of Cys-HB) to cyan and then to pinkish orange after irradiation was stopped. When exposed to oxygen, cyan and pinkish orange changed back to bluish purple, indicating that both of the two intermediates of cyan and pinkish orange were oxidized by oxygen to return to Cys-HB and could be ascribed to Cys-HB$^{\bullet -}$ and Cys-HBH$_2$, respectively. The further identification of the intermediates in terms of color will be made spectrophotometrically below.

3.2. Spin counteraction of TEMPO by the semiquinone anion radical of Cys-HB

The semiquinone anion radical of Cys-HB couldn't be detected by ESR technique by photolysis of deoxygenated of Cys-HB (1 mM) in water or in acidic DMSO-buffer (1:1 by volume, pH 5.6) in the absence or presence of electron donors. In the presence of electron donor such as NADH (5 mM), the color of the sample changed from bluish purple (Cys-HB) to pinkish orange (Cys-HBH$_2$) directly, and then back to bluish purple (Cys-HB) when exposed to oxygen, indicating that the hydroquinone of Cys-HB was formed during irradiation. In order to determine whether Cys-HB$^{\bullet -}$ generated in water or in acidic solution, the spin counteraction of TEMPO was adapted in terms of the fact that the intensity of TEMPO signal detected by ESR would decrease exponentially in the presence of Cys-HB$^{\bullet -}$ via the reaction shown in Eq. (6).

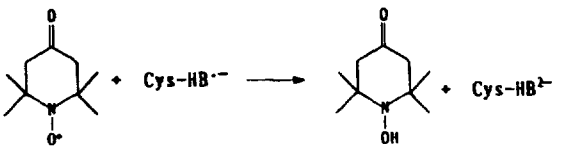

(6)

When the deoxygenated neutral buffer solution (pH 7.4) (Fig. 6A) or acidic DMSO-buffer (1:1 by volume, pH 5.6) solution (Fig. 6B) of Cys-HB (1 mM) and TEMPO (50 μM) were irradiated, the ESR signal intensity of TEMPO radical decreased exponentially with the irradiation time. This process could be promoted by the addition of electron donor such as NADH (5 mM) (Fig. 6C). The presence of oxygen inhibited the spin counteraction of TEMPO (Fig. 6D). This results suggested that Cys-HB$^{\bullet -}$ was produced in neutral buffer solution and acidic DMSO-buffer solution. And the decrease in Cys-HB concentration slowed down the spin counteraction of TEMPO (Fig. 6E).

The inability of ESR to detect Cys-HB$^{\bullet -}$ in neutral buffer or acidic media was caused by the shortening of the lifetime of Cys-HB$^{\bullet -}$. The decreased stability was considered to result from the accelerated second electron transfer (Eq. (8)) as well as the disproportionation process (Eq. (9)) catalyzed by protonation of the anion radical (Eq. (7)) at low pH [24] or in buffered solution [25]. These observations demonstrated that Cys-HB was photodynamically active even in aqueous system or in acidic system in terms of Type I mechanism.

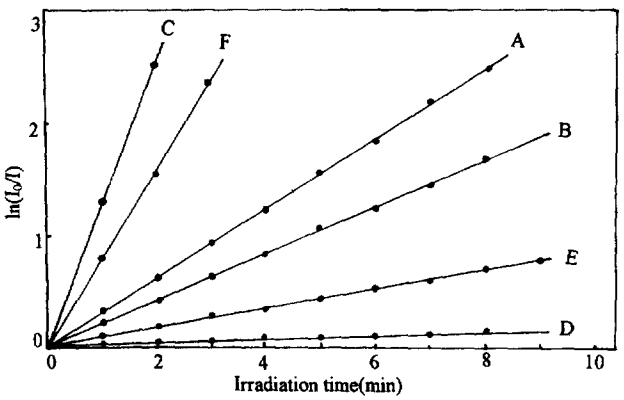

Fig. 6. Spin counteraction of TEMPO by Cys-HB photosensitization measured by the decrease of TEMPO signal intensity (I) in aqueous solution or acidic media. (A) Cys-HB (1 mM) in deoxygenated buffer solution(pH 7.4). (B) Cys-HB (1 mM) in deoxygenated acidic DMSO-buffer (1:1 by volume, pH 5.6) solution. (C) As in (A) but in the presence of NADH (5 mM). (D) Cys-HB (0.1 mM) in aerated buffer solution(pH 7.4). (E) Cys-HB (0.1 mM) in deoxygenated buffer solution (pH 7.4). (F) Cys-HB (1 mM) in deoxygenated DMSO.

$$\text{Cys-HB}^{\bullet -} + \xrightarrow{H^+} \text{Cys-HBH}\bullet \quad (7)$$

$$\text{Cys-HBH}\bullet \xrightarrow{D,H^+} \text{Cys-HBH}_2 \quad (8)$$

$$\text{Cys-HBH}\bullet + \text{Cys-HB}^{\bullet -} \xrightarrow{H^+} \text{Cys-HBH}_2 + \text{Cys-HB} \quad (9)$$

3.3. Spectrophotometric measurements on deoxygenated solutions of Cys-HB and cysteine

The absorption maximums of Cys-HB in DMSO-buffer (1:1 by volume, pH 8 and pH 11) solution are at 538 nm, 623 nm and 678 nm owing to the dissociation of the phenolic hydroxyls of Cys-HB in alkaline solution. The color of the sample containing Cys-HB and electron donor underwent the changes from bluish purple to cyan during irradiation and then to pinkish orange after irradiation was stopped (see above). To identify both of the intermediates of cyan in color and pinkish orange in color further, the spectrophotometric measurements were carried out and the comparison with HB was made at the same time.

3.3.1. Photoinduced reduction of Cys-HB in weak alkaline media

When a deoxygenated DMSO-buffer (1:1 by volume, pH 8.0) solution containing Cys-HB (60 μM) and cysteine (5 mM) was irradiated, the color of the sample changed from bluish purple to cyan during irradiation and then to pinkish orange after irradiation was removed, accompanied by the

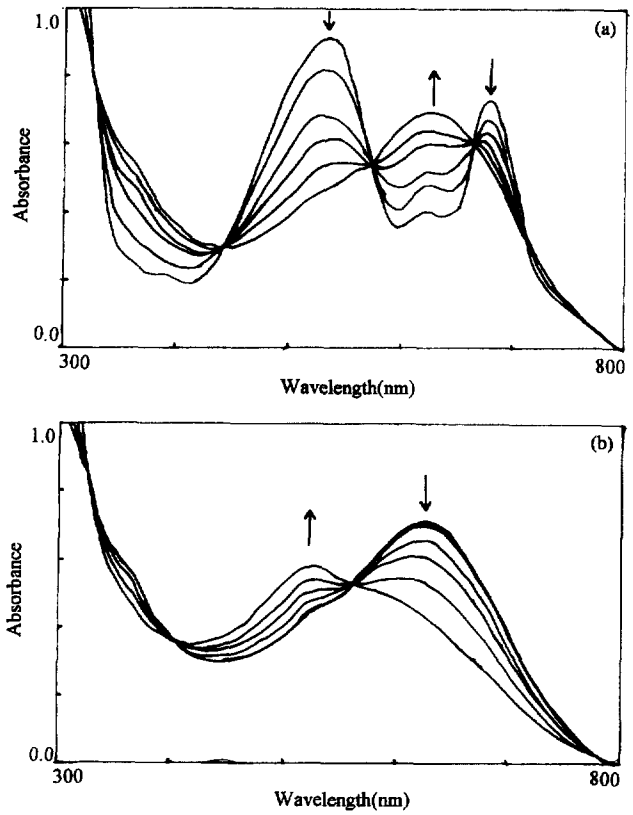

Fig. 7. Absorption spectra from deoxygenated DMSO-buffer (1:1 by volume, pH 8.0) solution containing Cys-HB (60 μM) and cysteine (5 mM) upon irradiation for (a) 0, 5, 10, 20, 40, 70 s, and (b) 120, 180, 300, 600, 900 s. The arrows indicate the direction of changes.

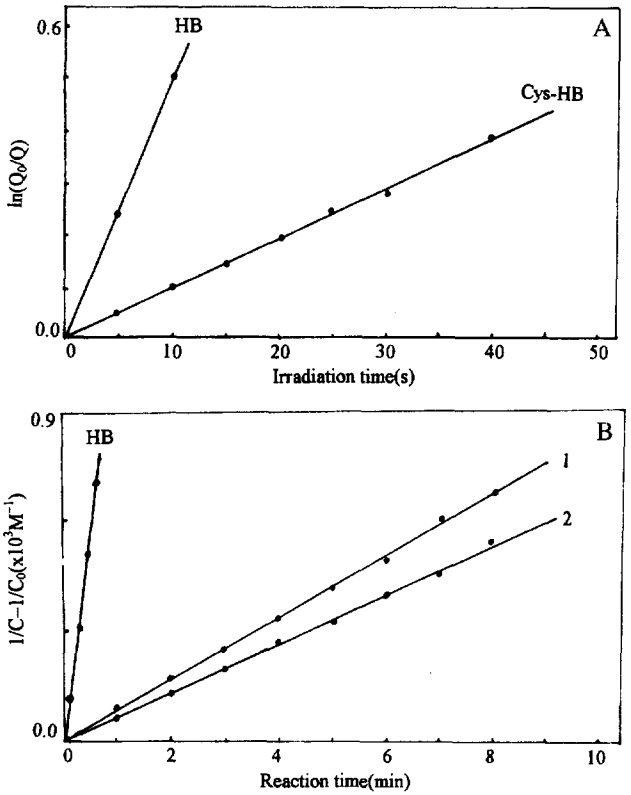

Fig. 8. (A) Dependence of the natural logarithm of the Cys-HB concentration (Q) on the irradiation time. When the deoxygenated DMSO-buffer (1:1 by volume, pH 8.0) solution of Cys-HB (60 μM) and cysteine (5 mM) was irradiated. (B) Dependence of the reciprocal of the Cys-HB semiquinone anion radical concentration (C) on the irradiation time (line 1) and on the dark reaction time (line 2) after (A).

generations of two reduced intermediates (see above). Fig. 7A and B showed the absorption curves recorded during the irradiation. It can be seen that the height of the absorption bands of Cys-HB at 538 nm and 678 nm decreased and a new broad band of the intermediate of cyan in color at 623 nm appeared, accompanied by three isobestic points at 440 nm, 576 nm and 640 nm (Fig. 7A). On further irradiation of the intermediate, another new absorption band at 504 nm was formed while the height of the absorption band at 623 nm decreased with the isobestic points at 404 nm and 562 nm (Fig. 7B), with the appearance of the intermediate of pinkish orange. These indicated that only two species were present in the system, i.e., Cys-HB and the intermediate of cyan in color shown in Fig. 7A, and the intermediate of cyan in color and that of pinkish orange in color shown in Fig. 7B, respectively. When exposed to oxygen during irradiation, both of the cyan and pinkish orange intermediates disappeared, suggesting that the two intermediates were the same as those observed by ESR spectra. The intermediate of cyan could be ascribed to Cys-$HB^{\bullet -}$, in good agreement with the identification by ESR measurement. In terms of the natural hypocrellin B, the maximum of $HB^{\bullet -}$ and HBH_2 was at about 618–628 nm and 502–520 nm dependent on the media, respectively [15,20,23,25,26]. Therefore the intermediate of pinkish orange could be ascribed to Cys-HBH_2 in accordance with the above observations and the reactions shown in Eqs. (5) and (6). It is very interesting that the absorption maximums of Cys-$HB^{\bullet -}$ and Cys-HBH_2 were similar to those of HB [15,23,26] and even to those of some other hypocrellin derivatives [25,27], and these suggested to some extent that the semiquinone anion radical and hydroquinone of hypocrellins and their derivatives were of the similar spectrophotometric characteristics.

In addition, the kinetics of the generation of Cys-$HB^{\bullet -}$ and Cys-HBH_2 was surveyed and the results were shown in Fig. 8A and B. Fig. 8A showed the plot of the natural logarithm of Cys-HB concentration vs. irradiation time measured by the absorbance at 538 nm. Fig. 8B showed the plot of the reciprocal of Cys-$HB^{\bullet -}$ concentration vs. irradiation time (line 1) and that vs. the dark reaction time (line 2), measured by the absorbance at 623 nm. It can be seen from Fig. 8A that the photogeneration of Cys-$HB^{\bullet -}$ in the presence of cysteine was consistent with first-order kinetics, confirming the pathway shown in Eq. (2). Fig. 8B suggested that the generation of Cys-HBH_2 during irradiation was instead consistent with second-order kinetics, interestingly, in agreement with the dark decay kinetics measured spectrophotometrically and by ESR method. These indicated that the generation of Cys-HBH_2 or the decay of Cys-$HB^{\bullet -}$ took place via Eq. (5)

predominantly rather than via Eq. (6), and was primarily independent of irradiation, and instead a thermodynamically controlled process.

3.3.2. Photoinduced reduction of Cys-HB in strong alkaline media

When the deoxygenated DMSO-buffer (1:1 by volume, pH 11.0) solution containing Cys-HB (60 μM) and cysteine (5 mM) was irradiated, Cys-$HB^{\bullet -}$ (λ_{max} 623 nm) and Cys-HBH_2 (λ_{max} 520 nm) were detected with the absorption spectrum changes similar to those for pH 8.0 (Fig. 7). The absorption band of Cys-HBH_2 shifted red from 504 nm at pH 8.0 to 520 nm at pH 11.0 owing to the dissociation of phenolic hydroxyl in Cys-HBH_2 in strong alkaline solution [25]. The kinetics of Cys-$HB^{\bullet -}$ and Cys-HBH_2 generation were shown in Fig. 10A and B, respectively. These observations indicated that the production of Cys-$HB^{\bullet -}$ and Cys-HBH_2 were more rapid than those in weak alkaline DMSO-buffer (1:1 by volume, pH 8.0) solution shown in Figs. 7 and 8, and consistent with first-order (Fig. 9A) and second-order kinetics (Fig. 9B), respectively. When Cys-HB was replaced by HB (40 μM), the spectrum changes shown in Fig. 10A demonstrated that $HB^{\bullet -}$ could not be detected and HBH_2 appeared directly. The generation of HBH_2 was consistent with first order kinetics primarily (Fig. 10B). TEMPO spin counteraction indicated that $HB^{\bullet -}$ was formed during irradiation of the deoxygenated DMSO-buffer (1:1 by volume, pH 11.0) solution of HB (40 μM) and cysteine (5 mM) (not shown). These results suggested that the generation of $HB^{\bullet -}$ (Eq. (10)) was the main controlling step compared with the generation of HBH_2 from $HB^{\bullet -}$ (Eq. (11)) owing to the significantly accelerated second-electron transfer as well as the disproportionation process (Eq. (11)) catalyzed by the destruction of the intramolecular hydrogen bond in HB [28] from the second dissociation of phenolic hydroxyl of HB in strong alkaline system [25]. The formation rate constants of $HB^{\bullet -}$, HBH_2, Cys-$HB^{\bullet -}$ and Cys-HBH_2 in alkaline media was listed in Table 2. As compared with $HB^{\bullet -}$, Cys-$HB^{\bullet -}$ was much more stable in strong alkaline media. This was tentatively attributed to the replacement of oxygen atom by nitrogen atom at 4 position on HB, which played a key role in increasing the stability of Cys-$HB^{\bullet -}$. The second dissociation in Cys-HB seldom occurred even up to pH 12 measured spectrophotometrically (He et al., unpublished data); the intramolecular hydrogen bonding remained in the structure of Cys-$HB^{\bullet -}$ (Fig. 11).

$$HB^{*}+D \rightarrow HB^{\bullet -}+D^{\bullet +} \quad (10)$$

$$HB^{\bullet -}+HB^{\bullet -} \rightarrow HBH_2+HB \quad (11)$$

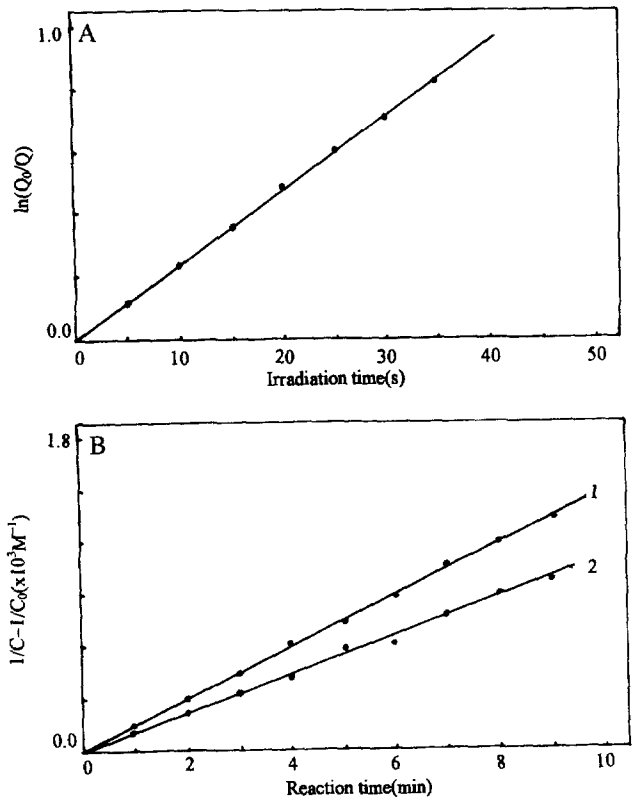

Fig. 9. (A) Dependence of the natural logarithm of Cys-HB concentration (Q) on the irradiation time. When DMSO-buffer (1:1 by volume, pH 11.0) solution of Cys-HB (60 μM) and cysteine (5 mM) was irradiated. (B) Dependence of the reciprocal of the Cys-HB semiquinone anion radical concentration(C) on the irradiation time (line 1) and on the dark reaction time (line 2) after (A).

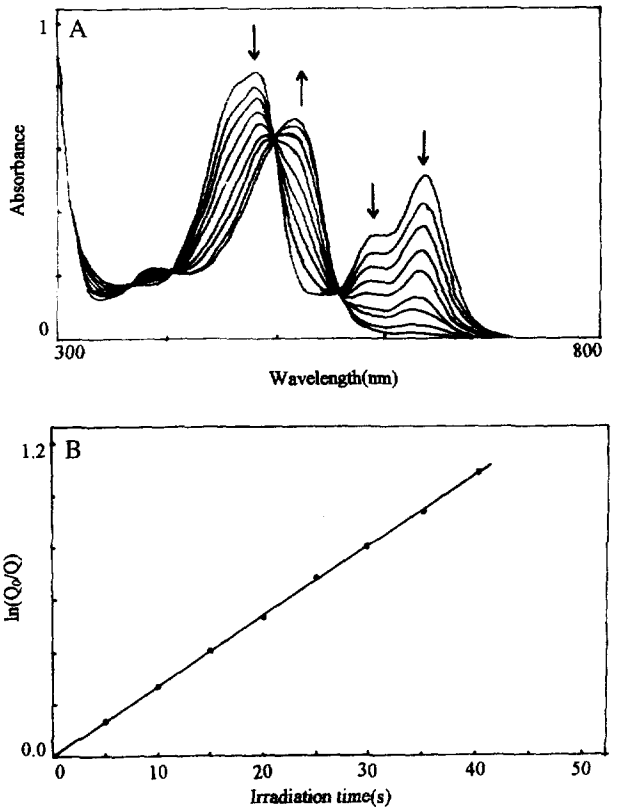

Fig. 10. (A) Spectrum changes recorded during irradiation of the deoxygenated (1:1 by volume, pH 11.0) containing HB (60 μM) and cysteine (5 mM) for 0, 5, 10, 20, 40, 100, 220, 520 and 1120 s. The arrows indicate the direction of changes. (B) Dependence of the natural logarithm of HB concentration (Q) on the irradiation time obtained according to (A).

Table 2
The formation rate constants of $HB^{\bullet -}$, HBH_2, Cys-$HB^{\bullet -}$ and Cys-HBH_2

pH	$HB^{\bullet -}$ (S^{-1})	HBH_2 ($M^{-1}\cdot S^{-1}$)	Cys-$HB^{\bullet -}$ (S^{-1})	Cys-HBH_2 ($M^{-1}\cdot S^{-1}$)
8.0	0.05	13.20	0.01	1.30
11.0	–	–	0.03	2.29

The DMSO-buffer (1:1 by volume, pH 8.0 or 11.0) solution of Cys-HB or HB (40 μM) and cysteine (5 mM) was irradiated. The production of the above four species was measured by the change in absorbance spectrophotometrically. These constants were estimated from Figs. 8 and 9.

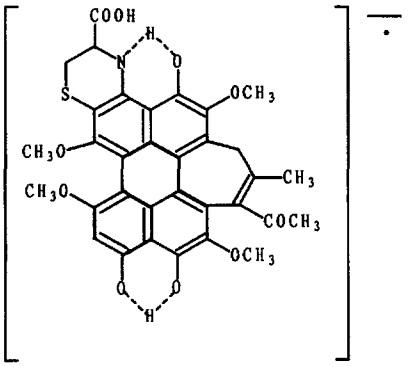

Fig. 11. Structure of the semiquinone anion radical of Cys-HB.

4. Conclusion

Illumination of Cys-HB in DMSO and DMSO-buffer (1:1 by volume, pH 8.0) solutions generated a strong ESR signal. This ESR signal was identified by the addition of the electron donors and the quenching of oxygen, confirmed by the spectrophotometric measurements, and ascribed to the semiquinone anion radical of Cys-HB (Cys-$HB^{\bullet -}$) rather than other species.

The generation of Cys-$HB^{\bullet -}$ in neutral buffer solution and acidic DMSO-buffer solution, which couldn't be detected by ESR or UV–Vis measurements, was detected by the spin trap of TEMPO, confirming that Cys-HB was photodynamically active in terms of Type I mechanism in aqueous solution or acidic media.

The spectrophotometric measurements of the photoinduced reduction of Cys-HB by cysteine in alkaline DMSO-buffer solution indicated that the absorption bands at 623 nm and 504 nm (or 520 nm) were ascribed to Cys-$HB^{\bullet -}$ and Cys-HBH_2 formed via first-order and second-order kinetics, respectively. The comparison with HB showed that Cys-$HB^{\bullet -}$ was much more stable and less susceptible in strong alkaline media than $HB^{\bullet -}$. This suggested that Cys-HB was a favorable Type I phototherapeutic agent with enhanced water solubility and absorbance in the domain of phototherapeutic window (600–900 nm).

Cys-HB photosensitized generation of active oxygen species ($^1O_2$, $O_2^{\bullet -}$ and HO•) has been investigated and discussed in another paper [29]. Superoxide radical ($O_2^{\bullet -}$) and hydroxyl radical (HO•) were detected by spin trapping of DMPO and the effects of inhibitors, such as SOD on the ESR signal of DMPO-$O_2^{\bullet -}$, and EtOH on that of DMPO•OH [29] Singlet oxygen ($^1O_2$) was detected by ESR method with 2,2,6,6-tetramethyl-4-piperidone (TEMP) as spin trap, and the quantum yield of $^1O_2$–generation (ϕ) was estimated to be 0.6 according to the 9.10-diphenyl-anthracene (DPA) bleaching method with ϕ for HB (0.76) as Ref. [29]. This indicates that Cys-HB is also a favorable Type I/II photosensitizer.

Acknowledgements

The research was supported by the Chinese National Science Foundation.

References

[1] L.J. Jiang. The structures, properties, photochemical reactions and reaction mechanisms of hypocrellin (I). Kexue Tongbao (1990) 1608–1616 and references cited therein.
[2] L.J. Jiang. The structures, properties, photochemical reactions and reaction mechanisms of hypocrellins (II). Kexue Tongbao (1990) 1681–1690 and references cited therein.
[3] Z.J. Diwu, J.W. Lown, Hypocrellins and their uses in photosensitization, Photochem. Photobiol. 52 (1990) 609–616 and references cited therein.
[4] Z.J. Diwu, J.W. Lown, Phototherapeutic potential of alternative photosensitizers to porphyrins, Pharmacol. Ther. 63 (1994) 1–35 and references cited therein.
[5] G.G. Miller, K. Brown, M. Ballangrud, O. Barajas, Z. Xiao, J. Tulip, J.W. Lown, J.M. Leithoff, M.J. Allalunis-Turner, R.D. Mehta, R.B. Moore, Preclinical assessment of hypocrellin B and hypocrellin B derivatives for photodynamic therapy of cancer: progress update, Photochem. Photobiol. 65 (1997) 714–722.
[6] J. Liu, G.G. Miller, L. Huang, Z.J. Diwu, J.W. Lown, J. Tulip, M.S. Mcphee, Synthesis and biodistribution of ^{14}C-radiolabelled hypocrellin B, J. Labelled Compd. Radiopharm. XXXVI (1995) 815–823.
[7] G.G. Miller, K. Brown, R.B. Moore, Z. Diwu, J. Liu, L. Huang, J.W. Lown, D.A. Begg, V. Chlumechy, J. Tulip, M.S. Mcphee, Intracellular uptake kinetics of hypocrellin photosensitizers for photodynamic therapy photosensitizers, SPIE Proc. 2371 (1995) 97–101.
[8] G.G. Miller, K. Brown, R.B. Moore, Z. Diwu, J. Liu, L. Huang, J.W. Lown, D.A. Begg, V. Chlumechy, J. Tulip, M.S. Mcphee, Intracellular uptake kinetics of hypocrellin photosensitizers for photodynamic therapy photosensitizers, Photochem. Photobiol. 61 (1995) 632–638.
[9] E.P. Estey, K. Brown, Z. Diwu, J. Liu, J.W. Lown, G.G. Miller, R.B. Moore, J. Tulip, M.S. Mcphee, Hypocrellins as photosensitizers for photodynamic therapy: a screening evaluation and pharmacokinetic study, Cancer Chemother. Parmacol. 37 (1996) 343–350.
[10] J.B. Hudson, J. Zhou, L. Harris, L. Yip, G.H.N. Towers, Hypocrellin, from *Hypocrella bambuase*, is phototoxic to human immunodeficiency viruses, Photochem. Photobiol. 60 (1994) 253–255.
[11] J.B. Hudson, V. Imperial, R.P. Haugland, Z.J. Diwu, Antiviral activities of photoactive perylenequinones, Photochem. Photobiol. 60 (1994) 253–255.
[12] Z.J. Diwu, J. Zimmermann, T. Meyer, J.W. Lown, Design, synthesis and investigation of mechanisms of action of novel protein kinase c inhibitors: perylenequinonoid pigments, Biochem. Pharmacol. 47 (1994) 373–385.
[13] T.G. Papazoglou, W.Q. Liu, A. Katsamouris, C. Fotakis, Laser-induced fluorescence detection of cardiovascular artherosclerotic deposits via their natural emission and hypocrellin probing, J. Pho-

tochem. Photobiol. B: Biol. 22 (1994) 139–144.
[14] Z.Y. Zhang, L.Y. Zang, G.R. Xu, N.B. Tao, D.H. Wang, Characteristics of the initial reactions during photosensitization of hypocrellin A, Sci. Sin. (B) 19 (1989) 361–367.
[15] E. Ben-Hur, A. Carmichael, P. Riesz, I. Rosenthal, Photochemical generation of superoxide radical and the cytotoxicity of phthalocyanines, Int. J. Radiat. Biol. 48 (1985) 837–846.
[16] Y.Z. Hu, L.J. Jiang, Characteristics of the reaction between semiquinone radical anion of hypocrellin A and oxygen in aprotic media, J. Photochem. Photobiol. A: Chem. 94 (1996) 37–41.
[17] J.Y. An, Y.Z. Hu, L.J. Jiang, Reactivity of semiquinone radical anions of hydroxyl perylenequinone with oxygen, J. Photochem. Photobiol. B: Biol. 33 (1996) 261–266.
[18] L.Y. Zang, B.R. Misra, H.P. Misra, Generation of free radical during photosensitization of hypocrellin A and their effects on cardial membranes, Photochem. Photobiol. 56 (1992) 453–462.
[19] K.H. Zhao, L.J. Jiang, Conversion of hypocrellin A in alkaline and neutral media, Youji HuaXue 9 (1989) 252–254.
[20] Y.Y. He, J.Y. An, W. Zhou, L.J. Jiang, Photoreaction of hypocrellin B and thiol compounds, J. Photochem. Photobiol. (1997), submitted.
[21] Y.Z. Hu, J.Y. An, L.J. Jiang, Studies of sulfonation of hypocrellin A and the photodynamic actions of the product, J. Photochem. Photobiol., B: Biol. 17 (1993) 195–207.
[22] K. Lang, M. Wagnerova, P. Stopka, W. Dameran, Reduction of dioxygen to superoxide photosensitized by anthraquinone-2-sulphonate, J. Photochem. Photobiol., A: Chem. 67 (1992) 187–195.
[23] Y.Z. Hu, J.Y. An, L.J. Jiang, D.W. Chen, Spectroscopic study on the photoreduction of hypocrellin A: Generation of semiquinone radical anion and hydroquinone, J. Photochem. Photobiol. A: Chem. 89 (1995) 45–51.
[24] K. Reszka, J.W. Lown, Photosensitization of anticancer agent. 8 one-electron reduction of mitoxantrone: an EPR and spectrophotometric study, Photochem. Photobiol. 50 (1989) 297–304.
[25] Y.Z. Hu, J.Y. An, L.J. Jiang, Spectroscopic studies of a soluble derivative of hypocrellin A and its one- and two-electron reduction products, Sci. Sin. (B) 37 (1994) 15–28 English edition.
[26] Y.Z. Hu, J.Y. An, L.J. Jiang, Studies on the photoinduced sulfonation of hypocrellins, J. Photochem. Photobiol. A: Chem. 70 (1993) 301–308.
[27] J.Y. An, L.J. Jiang, K.H. Zhao, The reduction and nucleophilic addition of mercaptoethanol to hypocrellin A, Chin. Sci. Bull. 37 (1992) 1274–1279 English edition.
[28] Z.J. Wang, M.H. Zhang, L.J. Jiang, Detection of the semiquinone anion radical of hypocrellin by ESR method, Huaxue Xuebao 50 (1992) 186–192.
[29] Y.Y. He, J.Y. An, L.J. Jiang, Photodynamic action of water-soluble hypocrellin derivative with significantly enhanced absorptivity in the PDT window II: photosensitized generation of active oxygen species, J. Photochem. Photobiol. B: Biol. (1998), submitted.